Effects of Homeopathic Phosphorus on *Encephalitozoon cuniculi*-Infected Macrophages In-Vitro

Mirian Yaeko Nagai[1] Luciane Costa Dalboni[1] Thayná Neves Cardoso[1] Michelle Sanchez Correia[1] Sandra Augusta G. Pinto[1] Andreia A. G. Pinto[1] Cideli de Paula Coelho[2,3] Anuska Alvarez-Saraiva[1] Giovani B. Peres[1] Maria Anete Lallo[1] Leoni Villano Bonamin[1]

[1] Research Center, Graduating Program of Environmental and Experimental Pathology, Universidade Paulista – UNIP, São Paulo, São Paulo, Brazil
[2] Universidade de Santo Amaro – UNISA, São Paulo, São Paulo, Brazil
[3] HD Science, São Caetano do Sul, São Paulo, Brazil

Address for correspondence Leoni Villano Bonamin, DVM, PhD, Research Center, Graduating Program of Environmental and Experimental Pathology, Universidade Paulista – UNIP, Rua Dr. Bacelar, 1212–4th floor, CEP 04026-002, São Paulo, SP, Brazil (e-mail: leonibonamin@gmail.com; leoni.bonamin@docente.unip.br).

Homeopathy 2019;108:188–200.

Abstract

Introduction *Encephalitozoon cuniculi* (*E. cuniculi*), a fungus that acts as an intracellular pathogen, causes a marked neurological syndrome in many host species and is a zoonotic concern. Although no well-established treatment for this syndrome is known, previous successful clinical experience using homeopathic phosphorus has been described in which symptom remission with no mortality occurred in 40/42 animals by means of unknown immunological mechanisms. The latter observation was the main motivation for this study.

Objective To verify, in an *in-vitro* model, if macrophages infected with *E. cuniculi* can change in function after treatment with different potencies of phosphorus.

Materials and Methods RAW 264.7 macrophages were infected with *E. cuniculi in-vitro* and treated with various homeopathic potencies of phosphorus. The vehicle was used as a control solution (0.06% succussed ethanol). After 1 and 24 hours, the following parameters were analyzed: parasite internalization (by the Calcofluor staining method), lysosome activity (by the acridine orange method), cytokine/chemokine production (by the MAGPIX system), and cell ultrastructure. Automatic image analysis was used when applicable, and the experiments were performed in triplicate.

Results Treatment with vehicle alone increased interleukin (IL)-6, tumor necrosis factor alpha and monocyte chemotactic protein -1 production ($p \leq 0.05$) and reduced the number of internalized parasites ($p \leq 0.001$). A progressive and time-dependent increase in RANTES (regulated on activation, normal T-cell expressed and secreted) and lysosome activity ($p \leq 0.002$) was observed only after treatment with the highest potency of phosphorus (*Phos* 200cH), together with decreased apoptosis rate, intense parasite digestion, and the presence of non-internalized spores.

Conclusions *Phos* 200 cH has a modulatory action on the activity of infected macrophages, especially a specific increase in RANTES, a key element in the prognosis of *E. cuniculi*-infected and of immunosuppressed patients bearing infections.

Keywords
- homeopathy
- fungus
- microsporidiosis
- cytokines
- chemokines

Leoni Villano Bonamin's ORCID is https://orcid.org/0000-0002-9850-9491.

received
November 7, 2018
accepted after revision
January 7, 2019
published online
April 18, 2019

DOI https://doi.org/10.1055/s-0039-1678700.
ISSN 1475-4916.

Introduction

The microsporidian *Encephalitozoon cuniculi* is an extremely important pathogen with zoonotic potential. This pathogen infects rabbits, causing severe and chronic granulomatous interstitial nephritis with fibrosis and granulomatous encephalitis.[1,2] Encephalitozoonosis in humans can cause local infections to spread systemically. The competence of the host's immune response and the fungus species involved are factors that determine the pathogenicity of the disease.[3–5] Rabbits can be infected with *E. cuniculi* via ingestion or inhalation of spores as well as by a trans-placental route. During the acute phase of the disease, which persists for an average of 30 days, the microsporidian replicates in the lungs, liver, and kidneys.[6] The clinical signs are classified into three groups: neuronal signals with vestibular syndrome (including head tilt), kidney failure, and eye injuries. Among the neuronal signals, vestibular syndrome, weakness, paresis of the hind limbs, and ataxia are often observed. The diagnosis is crucial to determine its possible zoonotic risks,[6,7] and there is no specific treatment for encephalitozoonosis.[7] Considering the difficulty associated with establishing an effective therapeutic protocol, the search for alternatives is critical. Several studies have demonstrated specific and relevant effects of homeopathic medicines in animals of different species under various nosological conditions;[8–10] nevertheless, the understanding of the general mechanisms through which such agents exert their effects is still very poor.[10]

Some previous clinical experience of one of the co-authors of this article was the main motivation for this study. Forty-two rabbits (*Oryctolagus cuniculus*), in which a diagnosis of encephalitozoonosis was established according to standard clinical parameters,[11,12] were treated daily with *Phosphorus* (*Phos*) 200 cH based on the traditional concept of "genus epidemicus" in which the three most important symptoms, ocular changes (including cataract, uveitis, hypopyon, and blindness), weakness of limbs and torticollis,[11,12] were used as the basis for this therapeutic choice. Based on the evolution of neuronal and renal signs, very good clinical outcome was obtained in all cases after 3 weeks of treatment. Of the 42 treated animals, 27 presented neurological signs (defined as head tilt, opisthotonus and tremors), and 18 presented renal signs such as hematuria, weight loss, and polyuria. Symptom remission was observed in 40/42 animals, with no mortality.

The second motivation for performing this *in-vitro* study was the previous establishment of a model for studying the effects of highly diluted substances in immune cells. Infection of macrophages *in-vitro* can provide a sensitive translational model for understanding the effects of highly diluted substances on the immune response. This model was previously validated by the results obtained in *Leishmania amazonensis*-infected macrophages treated with various homeopathic protocols,[13–15] which are related closely to observations obtained *in-vivo*. Using various models of macrophage challenge with other micro-organisms, our team has previously shown that highly diluted medicines, instead of killing the micro-organisms, facilitate the organization of a more effective pattern of macrophage response and arrest the parasite's life cycle.[8–10,13–23] For this reason, a similar model was designed herein to explain the clinical results, and avoiding new *in-vivo* experiments.

Materials and Methods

Preparation of Homeopathic Medicine, Quality Control, Treatment and Blinding

Phos matrix (*Phos* 5 cH, 29 cH or 199 cH) was prepared in a commercial pharmacy registered with the National Agency for Health Surveillance (ANVISA) according to the guidelines described in the Brazilian Homeopathic Pharmacopoeia, 3rd edition, 2011;[24] that is, sequential 1:100 dilutions followed by 100 succussions (vertical agitations) each using 30% ethanol solution and a mechanical Denise automatic arm (Autic; São Paulo, Brazil). In the terminology, the number represents the step of the sequential dilution, and cH refers to "centesimal Hahnemannian" or 1:100 dilution (proportion between active principle and solvent) followed by agitation according to the method described by Samuel Hahnemann.

The final working dilutions (*Phos* 6 cH, 30 cH and 200 cH) were prepared in our own laboratory 1 day prior to conducting the cell assays using pure water under sterile conditions. The control was the vehicle itself (30% ethanol) prepared at the same time using the same procedures, including a final 1:100 dilution in sterile pure water; thus, the final alcohol concentration was 0.06%. Before use in the cell cultures, the final dilution was filtered through a 0.22-µm filter (Millipore; Saint Louis, Missouri, USA), and the flasks were coded by staff not involved in the experimental laboratory to permit blinded procedures until the statistical analyses were completed.

Before the medicines were used in the experiments, rapid quality control testing was performed. Samples of each dilution were examined by scanning electron microscopy to permit the identification of suspended microparticles; the chemical nature of the samples was then analyzed using an energy dispersion spectroscopy system. Since contaminant micro- and nanoparticles are expected to be present in water,[25–29] this analysis was useful in eliminating any possibility that a predominant contaminating element was responsible for the effects described. The identification of suspended contaminant microparticles present in the tested solutions was performed using the micro-evaporation method followed by scanning electron microscopy under 10-kV working conditions and energy dispersive X-ray spectroscopy (JSM 6510; JEOL Ltd., Tokyo, Japan). Traces of Cl, Pr, Ca, Na, Zn, Si, Au, Pb and Al were randomly distributed among the analyzed particles ($n = 30$ per sample); the results showed that there was no predominant particulate contaminant that could produce false-positive results.

Following these steps, treatment of infected cells was performed according to the following design. To verify the step-wise internalization of fungi by macrophages, two experimental series were performed, the first after 1 hour

of infection and the second after 24 hours of infection. These times were chosen due to the rapid digestion activity of RAW 264.7 cells. In 24-well plates, 4 wells were treated with vehicle, *Phos* 6cH, *Phos* 30cH, and *Phos* 200cH, and 4 wells were untreated; 2 wells contained only macrophages, with no infection, these being data used to define the baseline values of each studied parameter and not included in the statistical analysis; 2 well plates were not used. The volume of the medicines and vehicle was equal to 20% of the total liquid volume in each well (500 µL); the total volume included 34 µL of *E. cuniculi* suspension + 100 µL medicine + 366 µL Roswell Park Memorial Institute (RPMI) medium enriched with 10% bovine fetal serum (BFS). The calculated final ethanol concentration was 0.06% in all treated wells. The proportion between medium and medicines was defined in a pilot study as a limit that did not cause osmotic stress in the cells.

Macrophage Culture and Infection

RAW 264.7 macrophages were purchased from the Cell Bank of Rio de Janeiro and kept frozen in a −80°C freezer. After thawing, they were expanded in cell culture bottles in RPMI medium (Cutilab; Campinas, Brazil) enriched with 10% BFS. When the confluence of the macrophage cultures reached 90%, the cells were washed with serum-free RPMI medium to remove any dead cells present in the supernatant. Then, 5 mL of RPMI medium was added, and the cells were detached using a cell scraper. A Pasteur pipette was used to remove the detached cells completely from the bottles. The cells were transferred to a Falcon tube, and their viability was determined using a Countess automatic counting system (Thermo Fisher; Camarillo, California, USA) after staining with 0.4% trypan blue dye. For plating the cells, round coverslips were placed in the 24-well sterile plates using one coverslip for each well.

The cells were held on ice and then centrifuged for 3 minutes at 333 g. The supernatant was discarded, and the pellet was homogenized in RPMI. After suspension, the cells were plated on coverslips (5×10^5 macrophages per coverslip) in 50 µL of RPMI. The cells were dispensed in the center of the coverslip and gently spread so that they were homogeneously distributed. Prior to incubation, 250 µL of RPMI enriched with 10% BFS was added to each well. The plate was incubated at 37°C for at least 2 hours to allow complete adherence of the macrophages. *E. cuniculi* spores were then added at a 2:1 ratio. The cells were treated at the moment of infection according to the protocol described in the section above.

Preparation of *E. cuniculi* Spores

E. cuniculi spores were previously cultured in RK-13 (rabbit kidney) cells. RK-13 cells were maintained in Eagle's medium (Cultilab; Campinas, Brazil) supplemented with penicillin-streptomycin (Sigma-Aldrich; Saint Louis, Missouri, USA) plus 10% BFS, 10% non-essential amino acids, and 10% pyruvate (Sigma-Aldrich; Saint Louis, Missouri, USA) and incubated at 37°C in 5% CO_2. Every 7 days, the culture supernatants were collected and centrifuged for 30 minutes at 500 g to obtain spores, which were stored at 4°C in 1x phosphate-buffered saline (PBS). Prior to infecting the cell cultures, the supernatants obtained from the cultures were pooled and purified. Briefly, 50% Percoll (Sigma-Aldrich; Saint Louis, Missouri, USA) diluted in PBS was added to the pellet pool, and the mixture was centrifuged for 20 minutes at 500 g. The supernatant containing the cell debris was discarded, and the pellet containing the spores was washed twice in PBS. *E. cuniculi* spores were counted in a Neubauer chamber[8] before their addition to macrophage cultures.

Analysis of Parasite Internalization

The number of parasites internalized by endocytosis and phagocytosis was measured from digital photomicrographs obtained using a fluorescence microscope (Olympus 60i; Tokyo, Japan). Non-fixed cells adhering to coverslips were stained using Calcofluor White stain (Sigma-Aldrich; Saint Louis, Missouri, USA) (10 µL per coverslip) 1 and 24 hours after infection and treatment.[30,31] In this method, the spores become blue and fluorescent due to the interaction of the dye with their chitin walls. Ten microscopic fields on each coverslip were recorded using a 40x objective; the captured images were analyzed using the manual counting tool in Offline MetaMorph software (Molecular Devices; San José, California, USA), and the number of internalized spores per macrophage was calculated. Two coverslips were used per treatment.

Determination of Cytokines and Chemokines

Culture supernatants were harvested at various times, centrifuged, and frozen at −80°C. The cytokine levels were measured using the MAGPIX—Luminex method (Kit e-Bioscience; Millipore, Saint Louis, Missouri, USA) according to the manufacturer's instructions. The kit permits the detection of the following cytokines: interleukin 1α (IL-1α), IL-1 β, interferon gamma (IFNγ), IL-10, IL-6, vascular endothelial growth factor A (VEGFA), tumor necrosis factor alpha (TNF-α), RANTES (regulated on activation, normal T cell-expressed and secreted) or CCL5, granulocyte-macrophage colony-stimulating factor (GM-CSF), IL-12-p40, IL-12-p70, macrophage inflammatory protein 1 (MIP-1β or CCL4), and monocyte chemoattractant protein-1 (MCP-1 or CCL2). Peptides that were present at levels below the detection limits of the method (defined in the manual provided by the manufacturer) were excluded from the statistical analysis. These samples were performed in quadruplicate.

Assessment of Lysosome Activity by Fluorescence Microscopy

After 1 and 24 hours, coverslips containing adherent macrophages infected with *E. cuniculi* were incubated with acridine orange dye for 20 minutes at 37°C to permit measurement of lysosome activity in real time. After incubation, the coverslips were washed in PBS and mounted on slides, using a drop of PBS as adherent. Quantitative analysis was performed automatically using offline MetaMorph software (Molecular Devices, USA); in this method, the intensity of the orange fluorescence exhibited by the vacuoles was measured. To ensure reliable results, the color filter of the software was

standardized and adjusted to reveal only fluorescence in the orange region (color model: HIS; hue: 19–20; intensity: 89–90). The principle of this method is based on the increase in the intensity of the orange fluorescence of the dye in acid medium. Ten microscopic fields on each coverslip were randomly measured using a 200x objective. This sample corresponds to 50% of the total area occupied by the adherent cells. This method was carried out in duplicate, two coverslips per treatment.

Transmission Electron Microscopy

When the experimenters were no longer blinded to the identity of the samples, a replication of the experiment was conducted, and two treatments (vehicle and *Phos* 200 cH) were chosen to be examined by transmission electron microscopy (TEM). In this experiment, the treatment was applied to cells in culture bottles rather than to cells in plates; after 24 hours of treatment, the cells were detached from the bottles using a cell scraper, fixed in 2% glutaraldehyde in cacodylate buffer (0.2 M, pH = 7.2) for 10 hours at 4°C and pooled in two microtubes, according to the treatment. After centrifugation (1,500 rpm for 5 minutes), the pellet at the bottom of each microtube was post-fixed in buffered 1% OsO_4 for 2 hours, treated with increasing concentrations of ethanol and embedded in Epon resin. The ultrastructural images were captured using a Tecnai G20 electron microscope (FEI Co., Hillsboro, Oregon, USA) with tomographic capacity and equipped with a high-resolution Eagle 4k x 4k camera.

Prior to electron microscopy, the material was examined in an optical microscope after the preparation of semi-thin sections stained with toluidine blue, aqueous uranyl citrate, and lead citrate. Thirty-five digital photomicrographs were registered from each treatment and the number of apoptotic cells was computed by MetaMorph software, using the manual counting option operated by two independent observers. Crescent-shaped nuclei, membrane blebs, and apoptotic bodies were the hallmarks used to identify them.

Statistical Analysis

Statistical analysis was performed using IBM SPSS version 21.0 and GraphPad Prism version 6.0 for Windows. Normality was assessed using the Shapiro–Wilk test and evaluated by inspection of quartile–quartile plots (Q–Q plots). The homogeneity of the variances was evaluated using the Levene test, and Welch correction was applied to analysis of variance (ANOVA) in cases of non-homogeneity. Outliers were evaluated by Q–Q plot inspection and removed if necessary. Each treatment was analyzed in duplicate or quadruplicate for all parameters analyzed, except the apoptotic cells counting, in which 35 fields per slide were used from pooled samples.

The results were evaluated through one-way ANOVA and Dunnett or Games–Howell's post-tests according to the case. The partial eta-square (η^2), a measure of effect size (from 0.1 to 1.0), has also been reported. This parameter is particularly useful for variables that present large deviation values and *p*-value analyses that could lead to type I errors (rejection of a null hypothesis when it is true) or type II errors (acceptance of a null hypothesis when it is not true). Values of partial η^2 higher than 0.4 were considered as relevant. Student "*t*" test was used to compare the number of apoptotic cells in control and *Phos* 200 cH treated cells, from the semi-thin sections.

The results are presented as the mean ± standard error, and values of $p < 0.05$ are considered to be significant. The figures were prepared using Prism 5.0 software.

Results

The time-dependent evolution of internalized microorganisms presented different patterns as a function of the treatment. As seen in ►**Fig. 1**, the number of internalized fungi was significantly reduced in all treated cultures after 1 and 24 hours of exposure, except in the case of samples treated with *Phos* 200 cH, in which reduction was significant only after 24 hours. Morphological analysis of the same samples

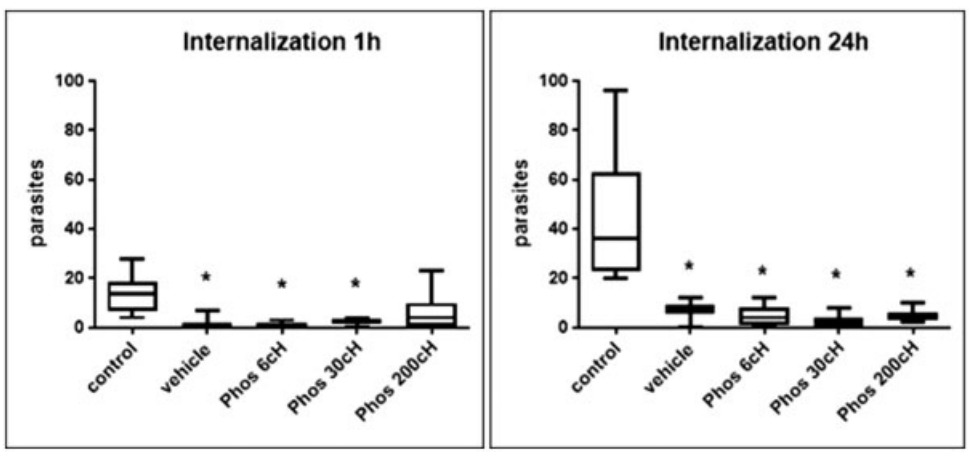

Fig. 1 Number of internalized *Encephalitozoon cuniculi* spores per macrophage measured using the Calcofluor White staining method and fluorescence microscopy. Counting was performed using Offline MetaMorph software and a manual counting system. After 1 hour: *ANOVA, Games–Howell, F (4, 25.422) = 9.663, $p < 0.001$, $\eta^2 = 0.486$ in relation to control. After 24 hours: *ANOVA, Games–Howell, F (4, 21.232) = 9.387, $p < 0.001$, $\eta^2 = 0.744$. The values shown are represented by a box-plot, with maximum and minimum limits. Control = untreated infected macrophages. ANOVA, analysis of variance.

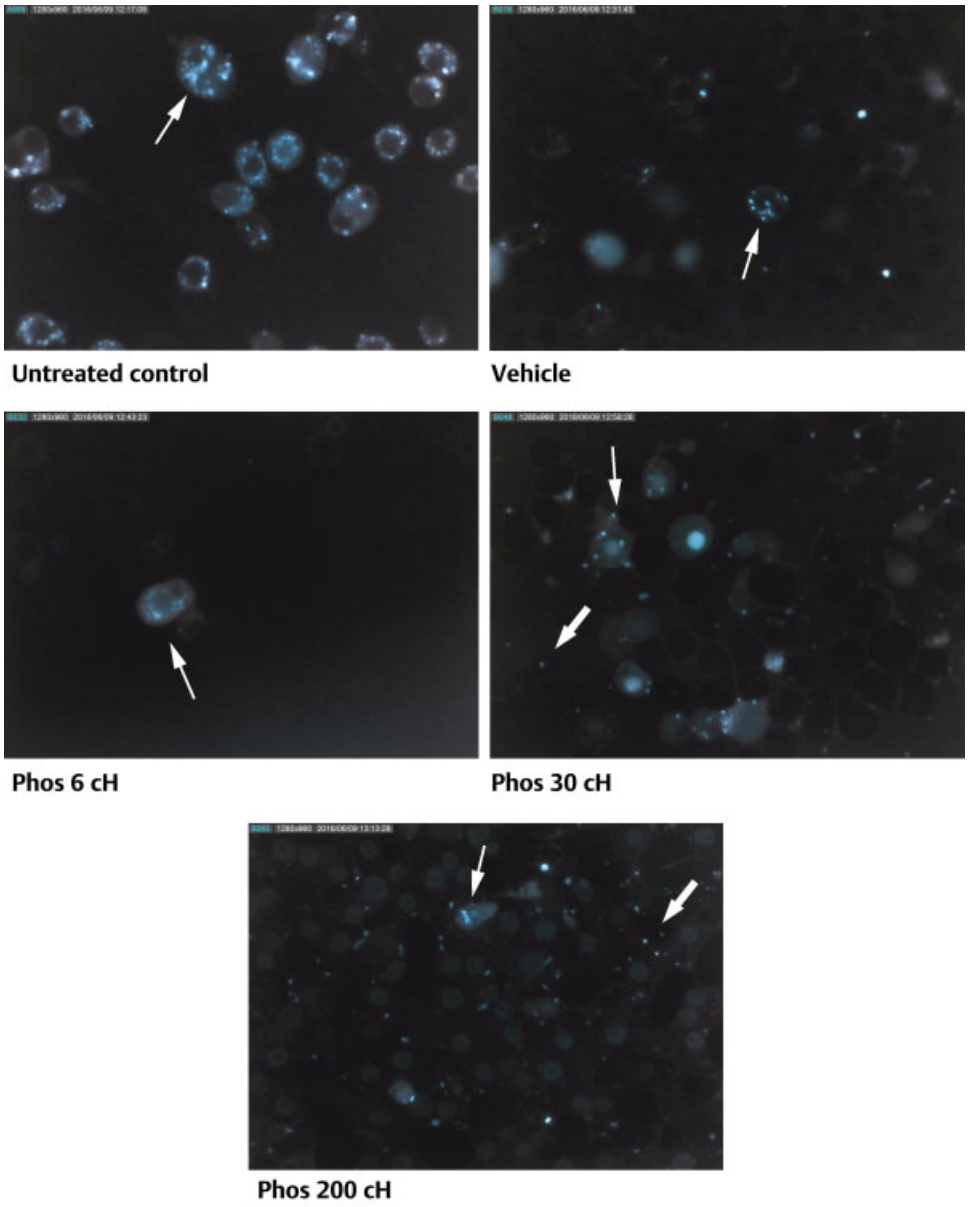

Fig. 2 Photomicrograph of coverslip-adherent macrophages 24 hours after infection with *Encephalitozoon cuniculi*. The samples shown include an untreated control, cells treated with vehicle, and cells treated with *Phos* at various dilutions. *Narrow arrows*: internalized spores; *large arrows*: non-internalized spores. The spores were stained by the blue fluorescent dye Calcofluor White due to their chitin walls. Objective: 200x.

after 24 hours of treatment showed a marked reduction in the number and size of internalized spores, reinforcing this finding (►**Fig. 2**). Moreover, the cultures treated with *Phos* 30 cH and 200 cH presented non-internalized spores (►**Fig. 2**).

The TEM and semi-thin toluidine-stained sections prepared after 24 hours of treatment corroborated these findings (►**Figs. 3** and **4**), showing two different patterns of parasite digestion in the cytoplasm. The vehicle-treated cells contained many easily recognized spores and debris within phagocytic vacuoles (►**Fig. 4A**). Apoptotic cells were seen in both the vehicle and *Phos* 200 cH-treated cultures; these cells presented a classical degeneration pattern including cell shrinkage, half-moon-shaped nuclei, chromatin condensation (►**Fig. 3**), and apoptotic body formation (►**Fig. 4B**). In the case of the *Phos* 200 cH cultures, much thinner and more delicate pathogen debris was found than in the control; moreover, empty vacuoles were frequently found (►**Fig. 4A**, **B**). An intermediate pattern was seen in vehicle-treated cells (►**Fig. 4C**). The quantitative analysis performed from the semi-thin sections revealed 23.00 $\pm$ 0.65 apoptotic cells per field in the vehicle treated cells and 17.28 $\pm$ 0.57 apoptotic cells in the *Phos* 200-cH treated cells ($p < 0.001$; degrees of freedom = 70).

The acridine orange assay showed increased size, distribution, and brightness intensity of fluorescent cytoplasmic vacuoles in cells treated with *Phos* 6 cH, 30 cH and 200 cH after 1 hour and in cells treated with *Phos* 200 cH after 24 hours relative to the respective controls. The quantitative analysis is shown in ►**Fig. 5**. A time-dependent increase in fluorescence intensity occurred after all treatments; greater

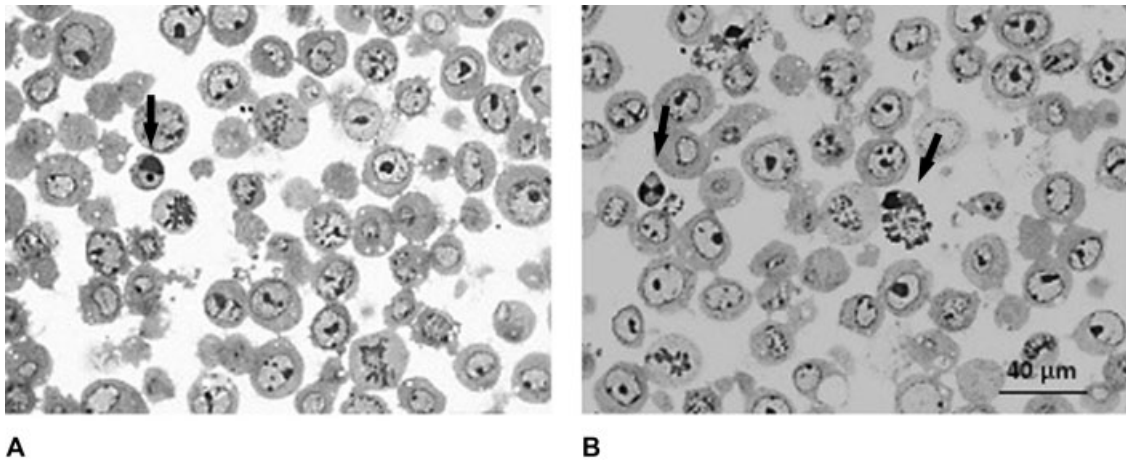

Fig. 3 Photomicrographs of semi-thin sections of infected macrophages after 24 hours. (**A**) Vehicle; (**B**) *Phos* 200 cH-treated cells. *Arrows*: apoptotic cells showing cell shrinkage, half-moon-shaped nuclei, and membrane blebs (apoptotic bodies). Toluidine stain. Objective: 100x.

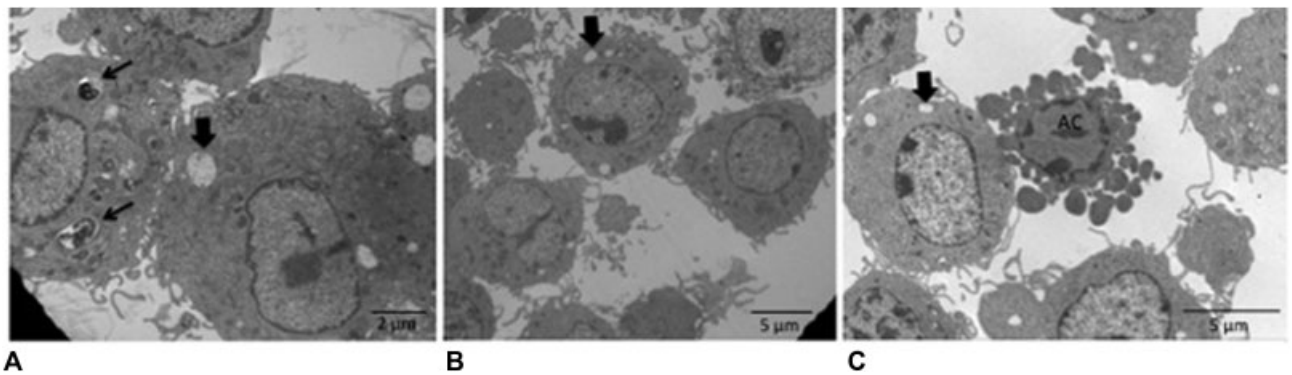

Fig. 4 Ultra-micrographs of macrophages infected with *Encephalitozoon cuniculi* and treated with vehicle or *Phos* 200 cH or not treated. (**A**) Vehicle-treated macrophages containing digestive vacuoles with spores undergoing lysis (narrow arrow) or without spores (large arrow); (**B**) Macrophages treated with *Phos* 200 cH containing digestive vacuoles (large arrow). (**C**) Vehicle-treated macrophages with digestive vacuoles (large arrow); an apoptotic cell (AC) is visible.

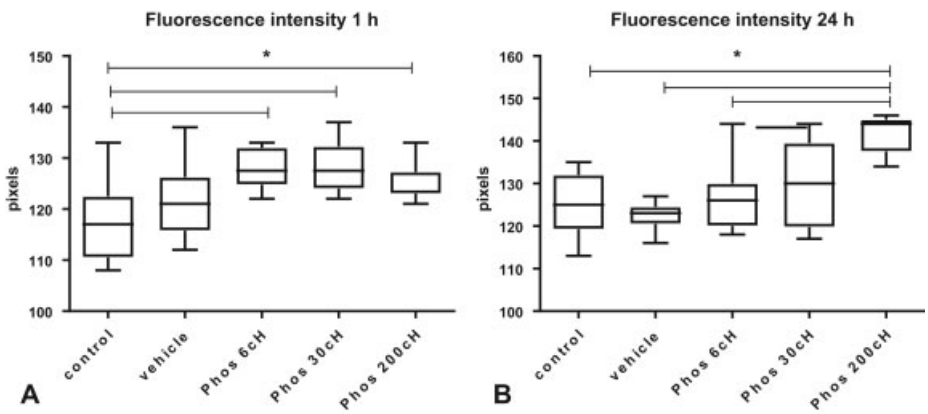

Fig. 5 Average fluorescence intensity (pixels) of macrophages stained with acridine orange and observed by fluorescence microscopy. The measurements were made using MetaMorph offline software and an automatic counting system. (**A**) *After 1 hour*: *ANOVA, Games–Howell, F (4, 23.653) = 6.060, $p = 0.002$, $\eta^2 = 0.390$ in relation to control. (**B**) *After 24 hours*: *ANOVA, Games–Howell, F (4, 21.150) = 53.624, $p < 0.001$, $\eta^2 = 0.522$. The values shown are represented by a box-plot, with maximum and minimum limits. ANOVA, analysis of variance.

variation was observed in cultures treated with *Phos* 6 cH and 30 cH, whereas treatment with *Phos* 200 cH resulted in a more stable effect. Illustrations of these differences are shown in ►**Figs. 6** and **7**.

The observed changes in cytokine and chemokine production were also time- and dilution-dependent. After 1 hour, there was a significant increase in IL-6 and TNFα in vehicle-treated cells, and the levels of these cytokines increased

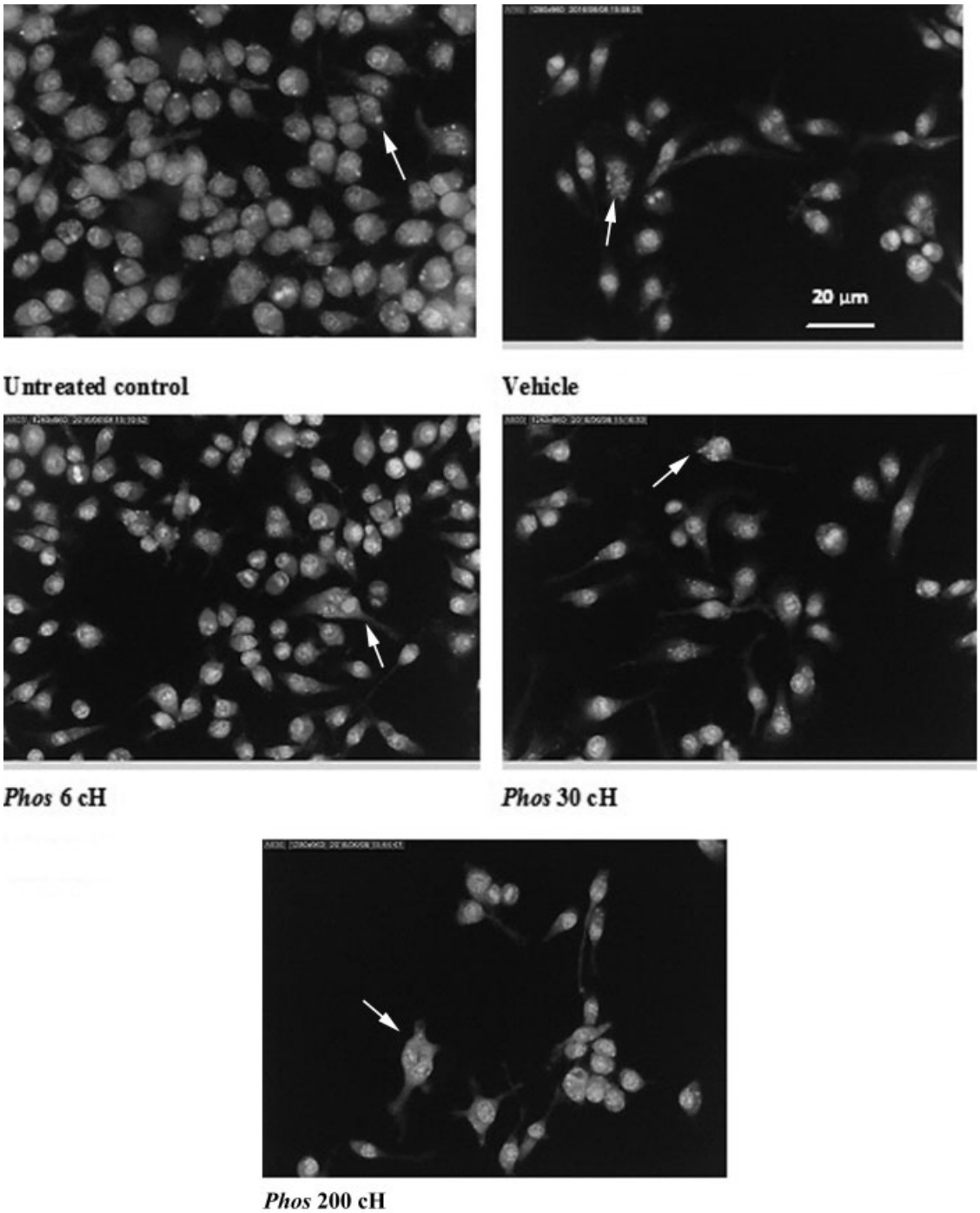

Fig. 6 Photomicrographs of coverslip-adherent macrophages 1 hour after infection with *Encephalitozoon cuniculi*: untreated control, cells treated with vehicle, and cells treated with *Phos* at various dilutions. The cytoplasm of the cells exhibits different degrees of brightness due to the orange fluorescence of lysosomes (*arrow*) after staining with acridine orange dye for 20 minutes at 37°C. Objective: 200x.

further after 24 hours of treatment (though the differences were not statistically significant due to the increase in variability). MCP-1, however, showed a very marked increase in all treated groups, including vehicle-treated cells, at both analyzed times; its concentration in the supernatant was nine-fold higher after 24 hours (►**Tables 1** and **2**). RANTES showed an important and significant increase in *Phos* 200 cH-treated cells after the first hour of treatment and a 10-fold increase after 24 hours. Treatment with lower dilutions resulted in intermediary values of RANTES at both times. The η^2 did not present relevant levels for RANTES at any tested potency after 24 hours (►**Tables 1** and **2** and ►**Fig. 8**).

Discussion

Cellular mechanisms related to the effects of homeopathic treatments have been well described in recent years and are related to the epigenetic control of specific genes, which

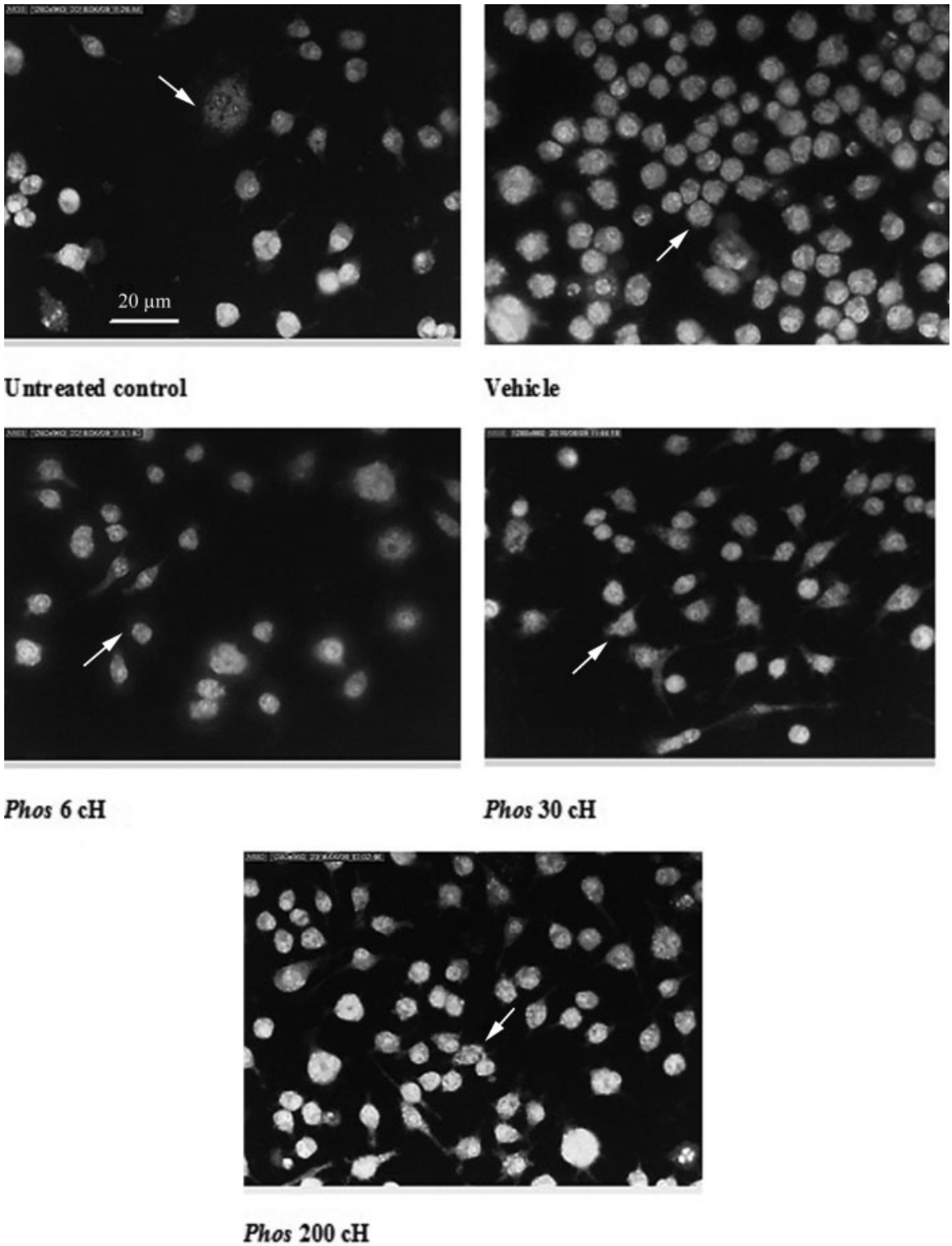

Fig. 7 Photomicrographs of coverslip-adherent macrophages 24 hours after infection with *Encephalitozoon cuniculi*: untreated control, cells treated with vehicle and cells treated with *Phos* at various dilutions. The cytoplasm of the cells exhibits different degrees of brightness due to the orange fluorescence of lysosomes (*arrow*) after staining with acridine orange dye for 20 minutes at 37°C. Objective: 200x.

depends on the nature of the medicine used and its dilution.[17,18,29,32–35] Based on our previous experience, macrophages respond to specific homeopathic stimuli by expressing specific cytokines and chemokines depending on the experimental context.[13,15] The choice of *Phos* to be used in this study was based on the classical homeopathic similia principle, since the main symptoms of encephalitozoonosis are listed in *Phos* materia medica and previous clinical observations reinforced the utility of this medicine for this kind of epidemiological problem.

The results show that the effects of the tested treatments can be classified into two categories: (1) effects related to the vehicle itself (increased levels of inflammatory cytokines and chemokines, mainly MCP-1); (2) effects related to treatment

Table 1 Concentrations of cytokines, chemokines and VEGF in the culture supernatants of macrophages infected with *Encephalitozoon cuniculi* and treated for 1 hour with various homeopathic dilutions of phosphorus

Peptide	Mean ± standard deviation					*p*-Value and η^2	
	Untreated control	Vehicle	*Phos* 6 cH	*Phos* 30 cH	*Phos* 200 cH		
IL-1α	14.08 ± 5.41	30.08 ± 7.80	2859.0 ± 16.6	25.95 ± 15.75	26.94 ± 17.52	0.786	0.135
IFNγ	4.94 ± 0.39	5.33 ± 0.56	4.45 ± 0.68	4.21 ± 0.76	5.50 ± 2.88	0.464	0.162
IL-6	3.52 ± 0.71	6.83 ± 1.69[a]	5.79 ± 0.65	5.55 ± 1.29	5.13 ± 0.46	0.035	0.582
IL-10	21.47 ± 8.40	51.98 ± 26.02	49.57 ± 19.93	45.78 ± 24.26	50.09 ± 29.08	0.602	0.191
IL-12p40	6.23 ± 1.04	6.61 ± 2.46	5.70 ± 0.48	4.96 ± 0.55	5.95 ± 3.06	0.502	0.134
IL-12p70	8.10 ± 3.05	17.43 ± 13.12	16.69 ± 8.04	14.34 ± 8.32	5.04 ± 2.14	0.332	0.319
MCP-1	717.5 ± 21.92	1816.0 ± 128.2[a]	1942.0 ± 228.9[a]	1633.75 ± 131.20	1774.33 ± 721.21[a]	< 0.001	0.629
MIP-1β	6036.0 ± 1193.5	10959.0 ± 816.6	10087.75 ± 732.64	8896.75 ± 633.61	7624.0 ± 5719.3	0.062	0.358
RANTES	8.49 ± 1.55	14.17 ± 4.09	14.17 ± 4.09	11.64 ± 2.85	21.65 ± 4.01[a]	0.054	0.574
VEGF	2.65 ± 0	3.06 ± 0.41	3.13 ± 0.13	2.93 ± 0.33	3.01 ± 0.83	0.769	0.131
TNFα	1887.0 ± 57.9	2320.5 ± 177.4[a]	2374.75 ± 331.05	2208.75 ± 99.66	1865.0 ± 1071.8	0.046	0.359

Abbreviations: IFNγ, interferon gamma; IL-6, interleukin 6; MCP-1, monocyte chemotactic protein-1; MIP-1β, macrophage inflammatory protein 1β; RANTES, regulated on activation, normal T-cell expressed and secreted; TNF-α, tumor necrosis factor alpha; VEGF, vascular endothelial growth factor.
Note: The values shown represent the mean and standard deviation, the level of significance, and eta-squared (effect size, η^2).
[a]ANOVA, Games-Howell in relation to control.

with specific potencies of *Phos* (changes in lysosome activity after 1 and 24 hours of treatment, reduced apoptosis rate and a progressive increase in RANTES/CCL5 between 1 hour and 24 hours relative to the controls), associated with the presence of non-internalized parasites.

The biological meaning of these effects can be understood in the context of recent findings on the pathogenesis of *E. cuniculi* infection. The balance between the increased digestion of internalized spores and the presence of non-internalized spores, even after 24 hours, suggests that macrophages treated with *Phos* 200 cH were able to phagocytoze and digest the parasites more efficiently than control cells, thereby inhibiting the phagocytosis-independent *E. cuniculi* internalization, which is the primary route of cell infection.[3,36,37] After ingestion, changes in pH and osmotic pressure cause the polar tube and sporoplasm to be ejected from the spore, with subsequent penetration of the host cell by the parasite.[36,38,39] Another means through which spores gain access to the host cell cytoplasm is endocytosis. If a spore is phagocytozed by a host cell, the polar tube can pass through the phagocytic vacuole membrane, delivering the sporoplasm into the host cell cytoplasm. Then, the parasite can manipulate host-cell death mechanisms as a way of perpetuating its survival.[36,37] In our

Table 2 Concentrations of cytokines, chemokines and VEGF in the culture supernatants of macrophages infected with *Encephalitozoon cuniculi* and treated for 24 hours with various homeopathic dilutions of phosphorus

Peptide	Mean ± standard deviation					*p*-Value and η^2	
	Untreated control	Vehicle	*Phos* 6 cH	*Phos* 30 cH	*Phos* 200 cH		
IL-1α	78.19 ± 4.78	56.09 ± 26.46	72.69 ± 1.83	84.50 ± 11.31	90.01 ± 11.46	0.332	0.562
IFNγ	5.97 ± 0.22	4.02 ± 1.86	5.58 ± 1.33	6.59 ± 2.54	7.30 ± 2.56	0.406	0.332
IL-6	5.40 ± 0.27	20.36 ± 5.76	10.64 ± 6.30	23.04 ± 17.55	26.67 ± 9.28	0.191	0.461
IL-10	48.01 ± 2.20	46.59 ± 25.81	49.64 ± 16.18	54.69 ± 30.09	51.73 ± 26.98	0.994	0.022
IL-12p40	5.56 ± 0.29	5.02 ± 1.42	5.46 ± 1.40	5.92 ± 2.08	8.55 ± 2.58	0.222	0.438
IL-12p70	5.37 ± 0.80	3.88 ± 0.88	6.82 ± 3.50	7.86 ± 3.63	6.01 ± 1.25	0.428	0.321
MCP-1	4981.0 ± 1544.3[a]	9025.66 ± 411.07	9406.66 ± 1287.16	9736.0 ± 1681.3	9752.66 ± 1096.79	0.014	0.717
MIP-1β	16289.5 ± 331.6	14912.0 ± 2834.0	15956.66 ± 1472.71	16640.66 ± 1302.29	16252.67 ± 395.93	0.752	0.175
RANTES	84.28 ± 1.28	218.66 ± 163.22	113.38 ± 13.50	252.66 ± 165.71	292.66 ± 122.83	0.084	0.378
VEGF	2.65 ± 0.26	2.86 ± 0.32	3.00 ± 0.48	2.91 ± 0.47	3.03 ± 0.42	0.864	0.121
TNFα	3154.0 ± 216.3	2207.0 ± 936.0	7030.0 ± 5963.9	2619.0 ± 895.7	2735.66 ± 367.45	0.450	0.384

Abbreviations: IFNγ, interferon gamma; IL-6, interleukin 6; MCP-1, monocyte chemotactic protein-1; RANTES, regulated on activation, normal T-cell expressed and secreted; TNF-α, tumor necrosis factor alpha; VEGF, vascular endothelial growth factor.
Note: The values shown represent the mean and standard deviation, the level of significance and eta-squared (effect size, η^2).
[a]ANOVA, Games-Howell in relation to the other groups.

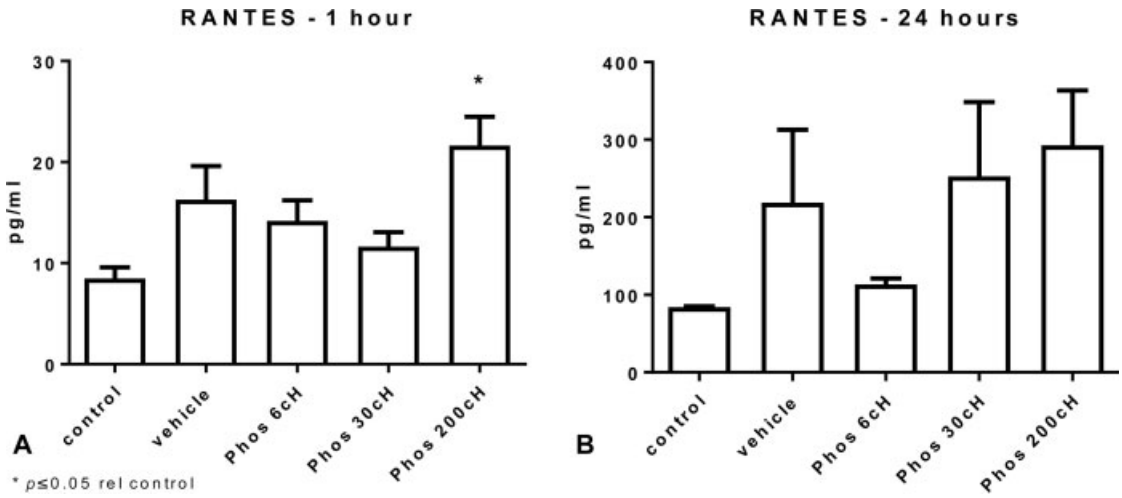

Fig. 8 Concentrations of relevant peptides in the culture supernatants of macrophages infected with *Encephalitozoon cuniculi* and treated for *1 hour* (**A**) or *24 hours* (**B**) with various homeopathic dilutions of phosphorus. (**A**) *ANOVA, Tukey, $F(4, 11) = 3.372$, $p = 0.05$, $\eta^2 = 0.574$ in relation to control. (**B**) ANOVA, Games–Howell, $F(4, 4.027) = 4.585$, $p = 0.084$, $\eta^2 = 0.378$. The values shown represent the mean and standard error. ANOVA, analysis of variance.

study, the absence of intact spores in cell vacuoles simultaneously with the marked presence of intercellular forms of the pathogen within macrophages, points to the efficacy of the microbicidal activity of treated macrophages, and a possible increase in the vulnerability of free spores to the host immune response, should the same effect be observed *in-vivo*.

In this sense, the presence of intact spores within macrophages following treatment could be related to a possible impairment of cell invasion. Two non-exclusive hypotheses can be considered: (1) the balance between the enhanced digestion of internalized spores and the presence of non-internalized spores, even after 24 hours of treatment with *Phos* 200 cH, might be caused by an improvement in phagocytosis and digestion of the parasites by the treatment, causing these processes to be more efficient than in the controls; (2) the treatment may inhibit the phagocytosis-independent *E. cuniculi* internalization pathway that represents the main pathway for cell infection.[3,36,37] The latter hypothesis could be related to a direct effect of the treatment on the surface structure of the spore that leads to a reduction in its rate of internalization. Moreover, the reduction in apoptotic cells after treatment with *Phos* 200 cH in relation to vehicle might represent reduction in macrophage susceptibility to the parasite mechanisms of corrupting cell functions and shows higher vitality of these cells, which could impact the intensity of lysosome activity.

With respect to chemokine production, MCP-1 (or CCL2) and RANTES were the most affected. MCP-1 attracts cells of the monocyte lineage to sites of inflammation and is tightly related to the pathogenesis of *E cuniculi* infection.[38,40] Instead, RANTES plays a critical role in determining the direction of inflammation after infection. RANTES is expressed by cells that play a crucial role in the homing and migration of memory T-cells during acute infections. Modifications in the function of RANTES (CCL5) and the RANTES receptor (CCR5) can lead to changes in prognosis due to dysfunctions in the CD8 T-cell response.[41] RANTES–CCR5 interaction promotes diapedesis and transmigration of Th1 cell types (but not Th2 cell types) through the endothelial layer at sites of inflammation and determines the type of immune response that occurs.[42] In the context of *E. cuniculi* infection, RANTES, among other chemokines (CXCL1, CXCL2, CXCL3, CXCL5, and CXCL8), plays an important role in granulocyte and T cell migration.[40] Patients infected with HIV1 who exhibit higher serum levels of RANTES are partially protected against the infection, indicating a better prognosis.[40,43] Herein, the specific increase in RANTES observed after treatment with *Phos* 200 cH is consistent with the biological context of *E. cuniculi* infection and could explain the clinical success of this therapy, as mentioned in "Introduction".

Analysis of the infected cells using a quantitative automatic method (MetaMorph) allowed us to determine the level of lysosome activity in the cells with high sensitivity. This finding, together with the ultrastructural findings, indicates the level of parasite digestion induced by the treatments. Thus, the vehicle-induced decrease in the number of internalized spores is probably related to increased parasite digestion, in contrast to the findings for *Phos* 200 cH-treated cells, in which complete parasite digestion was associated with reduction in the number of apoptotic cells and increase in non-internalized spores, suggesting changes in parasite pathogeny. The administration of vehicle alone also increased the levels of important inflammatory mediators such as IL-6 and MCP-1. The reason that the vehicle itself can produce pro-inflammatory responses could be related to the presence of the oxygen-rich nanobubbles that are found in highly agitated liquids, including homeopathic preparations;[44] thus, it could represent a general non-specific effect on cultured cells. All statistically significant data were related to a high "partial η^2" value (higher than 0.4), which reinforces the biological meaning of the results.

The effects of homeopathic medicines in relation to the vehicle (placebo) may be seen in studies performed *in-vivo* or

in standard clinical trials.[8,9,14–16,19–23] However, characterizing the specificity of such effects is even more important in refined studies designed *in-vitro*,[44] since it is known that the succussion itself can promote changes in the solvent organization, including the generation of different oxygen-derived radicals, mainly when water is used.[45–47] Macrophage cultures are very sensitive for detecting the effect of high dilutions but are also sensitive for detecting such solvent changes as well, concerning elements related to cell oxidative metabolism.[48–50] Such biochemical interference could lead to non-specific results—that is, not related to the Similia principle itself, but to the physico-chemical changes of the solvent due to agitation. Similar solvent-dependent effects can also be easily seen in vegetal models.[51,52] Thus, the comparison between the effects of succussed vehicle and the active homeopathic preparations in relation to a negative control is usually elucidative.

In the present work, differences comparing *Phos* 200cH and controls, in regard to parasite–phagocyte interaction, were shown by three complementary results: (1) the presence of higher numbers of non-internalized parasites for *Phos* 200cH than for the untreated control; (2) the acute production of RANTES in *Phos* 200cH in relation to the untreated control; and (3) the increase in lysosome activity, which presented clear statistical difference between *Phos* 200cH and vehicle itself, as shown in ►**Fig. 5**, associated with cell preservation or reduced apoptosis. These last findings are particularly important, indicating that eventual oxidative stress related to lysosomal function was clearly different between the treatments and cannot be related to a non-specific and biased outcome, secondary to the succussion of water. The findings (1) and (2) above are parasite and/or macrophage features, whose mechanisms need to be elucidated in further studies, though they are probably related to the specific expression of certain genes, as already seen in other similar studies using macrophages *in-vitro*.[17,18,48–50]

From a practical point of view, putative overlapping between the pro-inflammatory effects of succussed water, including the induction of inflammatory cytokines and chemokines (such as MCP-1, MIP-1β and TNFα) and the specific effects of *Phos* 200cH (acute expression of RANTES and lysosome activation), would also be present in clinical situations. Thus, an important consideration emerges: perhaps homeopathy acts through different and simultaneous mechanisms, with diverse degrees of specificity, which could be in accordance with the systemic effects observed in clinical practice.

In short, this study reveals some of the cell mechanisms involved in the action of *Phos* 200 cH on the experimental infection of macrophages with *E. cuniculi*, which would help to explain its clinical success in rabbits, as described above.

Conclusions

The *in-vitro* results presented in this work indicate putative mechanisms that underlie the clinical benefits of *Phos* 200 cH, as previously observed clinically in rabbits. Although non-specific, pro-inflammatory mechanisms that are related to the vehicle itself were observed, the specific action of *Phos* 200 cH was clearly related to increase in RANTES production, to lysosome activity, and to reduction in apoptosis of infected cells.

Highlights

- Successful previous clinical experience in rabbits diagnosed with encephalitozoonosis and homeopathically treated with high dilutions of phosphorus was the primary motivation for this study.
- An *in-vitro* model using infected macrophages was used in an attempt to identify the possible mechanisms involved.
- The results suggest non-specific, vehicle-related inflammatory action and that specific modulatory effects occurred at the highest potency of phosphorus (*Phos* 200 cH).
- The specific modulatory effects were related to an increase in RANTES production, decrease in apoptosis rate and an alteration in the balance between the phagocytic and endocytic pathways of parasite internalization by macrophages.

Conflict of Interest

There is no conflict of interest related to this project.

Acknowledgments

We thank CAPES-PROSUP for funding (Process No. 1586083). We thank Dr. Maria do Rocio Lázaro Rodrigues for the preparation of the drugs, Roberto Cabado and Gaspar Ferreira de Lima for TEM images, and Dr. Diva Denelle Spadacci-Morena for TEM image interpretation.

References

1 Rodríguez-Tovar LE, Villarreal-Marroquín A, Nevárez-Garza AM, et al. Histochemical study of *Encephalitozoon cuniculi* spores in the kidneys of naturally infected New Zealand rabbits. J Vet Diagn Invest 2017;29:269–277
2 Neumayerová H, Juránková J, Jeklová E, et al. Seroprevalence of *Toxoplasma gondii* and *Encephalitozoon cuniculi* in rabbits from different farming systems. Vet Parasitol 2014;204:184–190
3 Francisco Neto A, Dell'Armelina Rocha PR, Perez EC, et al. Diabetes mellitus increases the susceptibility to encephalitozoonosis in mice. PLoS One 2017;12:e0186954
4 Nell B, Csokai J, Fuchs-Baumgartinger A, Maaß G. *Encephalitozoon cuniculi* causes focal anterior cataract and uveitis in dogs. Tierarztl Prax Ausg K Klientiere Heimtiere 2015;43:337–344
5 Desoubeaux G, Peschke R, Le-Bert C, et al. Seroprevalence survey for microsporidia in common bottlenose dolphin (*Tursiops truncatus*): example of a quantitative approach based on immunoblotting. J Wildl Dis 2018;54:870–873
6 Wasson K, Peper RL. Mammalian microsporidiosis. Vet Pathol 2000;37:113–128
7 Abu-Akkada SS, Oda SS. Prevention and treatment of *Encephalitozoon cuniculi* infection in immunosuppressed rabbits with fenbendazole. Iran J Vet Res 2016;17:98–105
8 Bonamin LV, Endler PC. Animal models for studying homeopathy and high dilutions: conceptual critical review. Homeopathy 2010; 99:37–50

9 Bonamin LV, Cardoso TN, de Carvalho AC, Amaral JG. The use of animal models in homeopathic research–a review of 2010-2014 PubMed indexed papers. Homeopathy 2015;104:283–291
10 Bonamin LV. The soundness of homeopathic fundamental research. Revista de Homeopatia 2017;80:82–89
11 Jordan CN, Zajac AM, Lindsay DS. *Encephalitozoon cuniculi* infection in rabbits. Compend Contin Educ Vet 2006;28:108–116
12 Künzel F, Gruber A, Tichy A, et al. Clinical symptoms and diagnosis of encephalitozoonosis in pet rabbits. Vet Parasitol 2008; 151:115–124
13 de Santana FR, Dalboni LC, Nascimento KF, et al. High dilutions of antimony modulate cytokines production and macrophage – *Leishmania (L.) amazonensis* interaction in vitro. Cytokine 2017; 92:33–47
14 Nascimento KF, de Santana FR, da Costa CRV, et al. M1 homeopathic complex trigger effective responses against *Leishmania (L.) amazonensis* in vivo and in vitro. Cytokine 2017;99:80–90
15 Rodrigues de Santana F, de Paula Coelho C, Cardoso TN, et al. Modulation of inflammation response to murine cutaneous Leishmaniasis by homeopathic medicines: Antimonium crudum 30cH. Homeopathy 2014;103:264–274
16 Cajueiro APB, Goma EP, Dos Santos HAM, et al. Homeopathic medicines cause Th1 predominance and induce spleen and megakaryocytes changes in BALB/c mice infected with *Leishmania infantum*. Cytokine 2017;95:97–101
17 Olioso D, Marzotto M, Bonafini C, Brizzi M, Bellavite P. *Arnica montana* effects on gene expression in a human macrophage cell line. Evaluation by quantitative Real-Time PCR. Homeopathy 2016;105:131–147
18 Marzotto M, Bonafini C, Olioso D, et al. *Arnica montana* stimulates extracellular matrix gene expression in a macrophage cell line differentiated to wound-healing phenotype. PLoS One 2016;11: e0166340
19 de Paula Coelho C, Motta PD, Petrillo M, et al. Homeopathic medicine Cantharis modulates uropathogenic *E. coli* (UPEC)-induced cystitis in susceptible mice. Cytokine 2017;92:103–109
20 Bonamin LV, Bellavite P. Immunological models in high dilution research following M Bastide. Homeopathy 2015;104: 263–268
21 Rodrigues de Santana F, Coelho CdeP, Cardoso TN, Laurenti MD, Perez Hurtado EC, Bonamin LV. Modulation of inflammation response to murine cutaneous Leishmaniosis by homeopathic medicines: thymulin 5cH. Homeopathy 2014;103:275–284
22 Bonamin LV, Sato C, Zalla Neto R, et al. Immunomodulation of homeopathic thymulin 5CH in a BCG-induced granuloma model. Evid Based Complement Alternat Med 2013;2013:686018
23 Sato C, Listar VG, Bonamin LV. Development of broiler chickens after treatment with thymulin 5cH: a zoo technical approach. Homeopathy 2012;101:68–73
24 ANVISA. Farmacopeia Homeopática Brasileira 3ª edição 2011. Available at: http://portal.anvisa.gov.br/documents/33832/259147/3a_edicao.pdf/cb9d5888-6b7c-447b-be3c-af51aaae7ea8
25 Bell IR, Muralidharan S, Schwartz GE. Nanoparticle characterization of traditional homeopathically-manufactured *Gelsemium sempervirens* medicines and placebo controls. J Nanomedine Biotherapeutic Discov 2015;5:136. doi:10.4172/2155-983X.1000136
26 Chikramane PS, Suresh AK, Bellare JR, Kane SG. Extreme homeopathic dilutions retain starting materials: a nanoparticulate perspective. Homeopathy 2010;99:231–242
27 Chikramane PS, Suresh AK, Kane SG, Bellare JR. Metal nanoparticle induced hormetic activation: a novel mechanism of homeopathic medicines. Homeopathy 2017;106:135–144
28 Temgire MK, Suresh AK, Kane SG, Bellare JR. Establishing the interfacial nano-structure and elemental composition of homeopathic medicines based on inorganic salts: a scientific approach. Homeopathy 2016;105:160–172
29 Saha SK, Roy S, Khuda-Bukhsh AR. Ultra-highly diluted plant extracts of *Hydrastis canadensis* and *Marsdenia condurango* induce epigenetic modifications and alter gene expression profiles in HeLa cells in vitro. J Integr Med 2015;13:400–411
30 Desoubeaux G, Franck-Martel C, Caille A, et al. Use of Calcofluor-blue brightener for the diagnosis of *Pneumocystis jirovecii* pneumonia in bronchial-alveolar lavage fluids: a single-center prospective study. Med Mycol 2017;55:295–301
31 John DE, Nwachuku N, Pepper IL, Gerba CP. Development and optimization of a quantitative cell culture infectivity assay for the microsporidium *Encephalitozoon intestinalis* and application to ultraviolet light inactivation. J Microbiol Methods 2003; 52:183–196
32 Marzotto M, Olioso D, Brizzi M, Tononi P, Cristofoletti M, Bellavite P. Extreme sensitivity of gene expression in human SH-SY5Y neurocytes to ultra-low doses of *Gelsemium sempervirens*. BMC Complement Altern Med 2014;14:104
33 Olioso D, Marzotto M, Moratti E, Brizzi M, Bellavite P. Effects of *Gelsemium sempervirens* L. on pathway-focused gene expression profiling in neuronal cells. J Ethnopharmacol 2014;153:535–539
34 Khuda-Bukhsh AR, Sikdar S. Condurango 30C induces epigenetic modification of lung cancer-specific tumour suppressor genes via demethylation. Forsch Komplement Med 2015;22:172–179
35 Mondal J, Das J, Shah R, Khuda-Bukhsh AR. A homeopathic nosode, Hepatitis C 30 demonstrates anticancer effect against liver cancer cells in vitro by modulating telomerase and topoisomerase II activities as also by promoting apoptosis via intrinsic mitochondrial pathway. J Integr Med 2016;14:209–218
36 Ghosh K, Weiss LM. T cell response and persistence of the microsporidia. FEMS Microbiol Rev 2012;36:748–760
37 Scanlon M, Leitch GJ, Shaw AP, Moura H, Visvesvara GS. Susceptibility to apoptosis is reduced in the microsporidia-infected host cell. J Eukaryot Microbiol 1999;46:34–35
38 Han B, Polonais V, Sugi T, et al. The role of microsporidian polar tube protein 4 (PTP4) in host cell infection. PLoS Pathog 2017;13: e1006341
39 Desoubeaux G, Piqueras MDC, Pantin A, et al. Application of mass spectrometry to elucidate the pathophysiology of *Encephalitozoon cuniculi* infection in rabbits. PLoS One 2017;12:e0177961
40 Fischer J, West J, Agochukwu N, Suire C, Hale-Donze H. Induction of host chemotactic response by *Encephalitozoon* spp. Infect Immun 2007;75:1619–1625
41 Crawford A, Angelosanto JM, Nadwodny KL, Blackburn SD, Wherry EJ. A role for the chemokine RANTES in regulating CD8 T cell responses during chronic viral infection. PLoS Pathog 2011; 7:e1002098
42 Kawai T, Seki M, Hiromatsu K, et al. Selective diapedesis of Th1 cells induced by endothelial cell RANTES. J Immunol 1999; 163:3269–3278
43 Mutuiri SP, Kutima HL, Mwapagha LM, et al. RANTES gene polymorphisms associated with HIV-1 infections in Kenyan population. Dis Markers 2016;2016:4703854
44 Witt CM, Bluth M, Albrecht H, Weisshuhn TE, Baumgartner S, Willich SN. The in vitro evidence for an effect of high homeopathic potencies–a systematic review of the literature. Complement Ther Med 2007;15:128–138
45 Demangeat JL. Gas nanobubbles and aqueous nanostructures: the crucial role of dynamization. Homeopathy 2015;104:101–115
46 Madl P, Del Giudice E, Voeikov VL, et al. Evidence of coherent dynamics in water droplets of waterfalls. Water 2013;5:57–68
47 Voeikov VL. Fundamental role of water in bioenergetics. In: Belousov VL, Voeikov VK, Martynyuk VS, eds. Dordrecht: Springer; 2007:89–104
48 de Oliveira CC, Abud AP, de Oliveira SM, et al. Developments on drug discovery and on new therapeutics: highly diluted tinctures act as biological response modifiers. BMC Complement Altern Med 2011;11:101
49 Gonçalves JP, Dos Santos MLF, Rossi GR, Costa Gagosian VS, de Oliveira CC. Differential effects of Zincum metallicum on cell models. Homeopathy 2017;106:171–180

50 Bonafini C, Marzotto M, Bellavite P. In vitro effects of zinc in soluble and homeopathic formulations on macrophages and astrocytes. Homeopathy 2017;106:103–113
51 Barreto CS, Homsani F, Holandino C, Silva NCB. Plant tissue culture and ultra high diluted studies: suggesting a novel model using in vitro techniques. In: Proceedings of the XXX GIRI meeting; Sep 9–11, 2016; Amsterdam, The Netherlands. Int J High Dilution Res 2016;15:45–49
52 Otsuka I. Nanoscale cluster structure of O_2 gas-filled nanobubbles is O_2 gas-supersaturated alkaline solution. In: Proceedings of the XXIX GIRI meeting; June 3–5, 2015; Verona, Italy. Int J High Dilution Res 2015;14:40